*Int. J. Electrochem. Sci.*, 13 **(2018)** 6462 – 6472, doi: 10.20964/2018.07.49

International Journal of
ELECTROCHEMICAL
SCIENCE
www.electrochemsci.org

# Investigation on Corrosion Inhibition of Mild Steel by Sinapine Thiocyanate in $H_2SO_4$ Solution

*Xi lan Jiang[1], Chuan Lai[2], Zhen Xiang[2,*], Jing Tang[3], Lang Liu[2], Yun tian Gu[2], Ren shuang Wu[2], Zhi rong Wu[2], Jia jia Yuan[2], Dan qi Hou[2], Yu chao Zhang[2]*

[1] School of Chemistry and Chemical Engineering, Eastern Sichuan Sub-center of National Engineering Research Center for Municipal Wastewater Treatment and Reuse, Key Laboratory of Exploitation and Study of Distinctive Plants in Education Department of Sichuan Province, Sichuan University of Arts & Science, Dazhou 635000, PR China
[2] College of Chemistry and Environmental Engineering, Key Laboratories of Fine Chemicals and Surfactants in Sichuan Provincial Universities, Sichuan University of Science & Engineering, Zigong 643000, PR China
[3]Department of Medical Image and Examination, Dazhou Vocational and Technical College, Dazhou 635000, PR China
[*]E-mail: tougaolc@163.com

*Received:* 6 March 2018 / *Accepted:* 4 April 2018 / *Published:* 5 June 2018

Herein, the investigation on corrosion inhibition of mild steel in $H_2SO_4$ solution by green corrosion inhibitor of *Sinapine Thiocyanate* (GCI-ST) is presented. After GCI-ST isolated and purity determined, the corrosion inhibition of mild steel (MS) in $H_2SO_4$ solution with various concentration of GCI-ST was studied by potentiodynamic polarization, weight loss measurement and microstructure analysis. The study results indicate that GCI-ST can act as an effective green inhibitor, which is a mixed-type inhibitor, and the adsorption of GCI-ST on MS surface obeys Langmuir isotherm. In addition, it found that the inhibition efficiency increases with GCI-ST concentration increasing, decreases with $H_2SO_4$ concentration, temperature and storage time increasing.

**Keywords:** Semen raphani; Corrosion inhibition; Polarization; Mild steel.

## 1. INTRODUCTION

Up to now, a number of organic compounds have been reported as corrosion inhibitors for different metals in various aggressive environments [1-3]. But, unfortunately most of corrosion inhibitors are not only expensive but also toxic to living beings. Therefore, it is very important to

develop the green and cheap inhibitors. Most of the natural products are non-toxic, biodegradable and readily available in plenty. Over the past decades, many researchers have been reported using naturally occurring substances as green inhibitor for several metals in different corrosive solution. Different researchers [4-10] reported that the *Citrus aurantium, Juniperus procera, Sida acuta, Nicotiana tabacum, Chenopodium ambrosioides, Sida acuta, Spondias mombin L., Fuji apple peel, Tinospora crispa* leaves and stem extracts can act as the green inhibitors for steel in acid medium.

*Raphanus sativus L.*, an edible root vegetable of the brassicaceae family, has been cultivated all over the world. The dried ripe seed of *Raphanus sativus L.* (namely in Chinese "*Laifuzi*") is a traditional Chinese herbal medicine (TCM) recorded in Pharmacopoeia of China and has been extensively used in China and other countries for treatment of various diseases [11]. Previous phytochemical studies on *Raphanus sativus L.* indicated the presence of alkaloids [12], glucosinolates [13], isothiocyanates [14-15] and brassinosteroids [16-17]. Sinapine was the major bioactive alkaloids existed in the *Sinapine thiocyanate* and modern pharmaceutical studies showed that compound possessed various biological activities, including anti-inflammatory [18], antioxidative [19], radioprotective [20-21] and antiaging effects [22].

Different plants extracts as green inhibitors have been reported [3-10], however, the extracts of *Raphanus sativus L.* as green inhibitor for Q235 steel in HCl solution had been reported in our previous work [7] (*Int. J. Electrochem. Sci.*, 13 (2018) 3224 - 3234). As a more comprehensive evaluation on corrosion inhibition of GCI-ST in acid solution, the present work will exhibit an extension study on corrosion inhibition of mild steel in $H_2SO_4$ solution by the green corrosion inhibitor of *Sinapine Thiocyanate* (GCI-ST).

## 2. MATERIALS AND METHODS

### *2.1 Materials and general experimental procedures*

All the chemicals involving the concentrated sulfuric acid ($H_2SO_4$, 98%), potassium thiocyanate, methanol, ethanol, petroleum ether and ethyl acetate were all analytical grade and purchased from Chengdu Kelong Chemical Reagent Factory (Chengdu, China). The *semen raphani* used to isolate *Sinapine Thiocyanate* was purchased from Lotus Pond Chinese Herbal Medicine Market (Chengdu, China).

The all test specimens (2 mm×25 mm×50 mm, $S$=28.0 $cm^2$) and the working electrode (0.785 $cm^2$) were prepared by mild steel (MS) with the composition of C (0.165%), Si (0.268%), P (＜ 0.015%), S (＜0.011%), Mn (0.419%) and Fe (Bal.). Potentiodynamic polarization measurement was conducted by conventional three-electrode system consisting of MS working electrode, a saturated calomel reference electrode (SCE) and a counter Pt electrode employing the CHI 660D (Shanghai, China) electrochemical workstation to record Tafel polarization curve. The various concentrations of $H_2SO_4$ solution were diluted by 98% $H_2SO_4$with deionized water.

*2.2 Extraction and isolation*

The dried ripe seed of *Raphanus sativus L.* (10.0 kg) were convert to powder and extracted with EtOH (ethanol) for three times (20 L, 2d, 50°C, each). The solvent was evaporated, and the residue (1.5 kg) suspended in 90% MeOH (methanol) and then extracted with petroleum ether (3×3 L). After concentrating the 90% MeOH layer in vacuo, the residue (415.0 g) was suspended in deionized water and then extracted with ethyl acetate. The water layer fraction (295.0 g) was applied to an RP-$C_{18}$ column (10×55 cm, 1000 g), eluting with MeOH/$H_2O$ (10:90) to afford fractions 1-4. Fraction 2 (87.0 g) were mixing in 500 mL of 0.1 mM KSCN (potassium thiocyanate) solution and standing at 5°C until solid powder precipitate in the botton of the flask. *Sinapine thiocyanate* (GCI-ST, 10.3 g) was isolated from solid powder (13.5 g) by recrystallization in MeOH (see figure 1). Based on the analysis of reversed-phase high performance liquid chromatography and quantitive NMR (*Coumarin* as internal standard material), the *Sinapine thiocyanate* with the purity of 96.48% was obtained (section 3.1, Figure 2). White amorphous powder (MeOH); ESI-MS *m/z*： 310 ($[M\text{-}SCN]^+$), $^1$H-NMR (400 MHz, MeOD) $\delta$： 3.27 (9H, s, -N-$CH_3$), 3.80 (2H, m, H-11), 3.88 (6H, s, -O-$CH_3$), 4.66 (2H, m, H-10), 6.46 (1H, s, $J$ = 16.0 Hz, H-8), 6.94 (2H, s, H-2, 6), 7.67 (1H, d, $J$ = 16.0 Hz, H-7). $^{13}$C-NMR (100 MHz, DMSO-$d_6$) $\delta$： 53.5 (N-$CH_3$), 56.6 (3, 5-$OCH_3$), 58.6 (C-10), 64.7 (C-11), 106.9 (C-2, 6), 114.6 (C-8), 124.7 (C-1), 130.0 (C≡N), 139.1 (C-4), 146.7 (C-7), 148.5 (C-3, 5), 166.4 (C-9). Based on the above evidences and compared with the known compounds [23], which is in good agreement the structure of GCI-ST showing in figure 1.

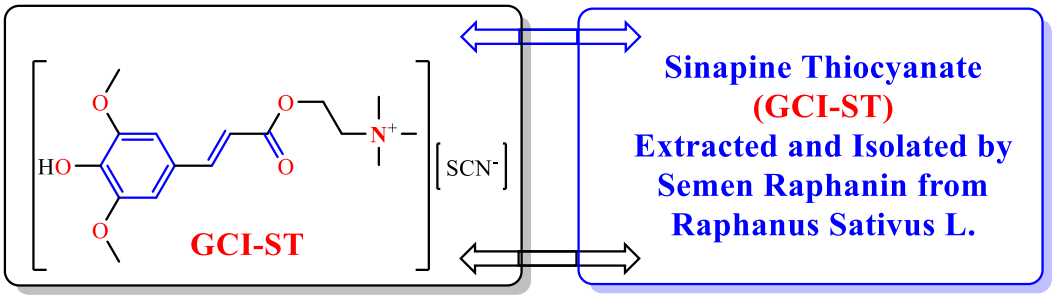


**Figure 1.** Chemical structure of GCI-ST.

*2.3 Corrosion inhibition performance evaluation*

*Weight loss measurement* [24-25]: According to this method, the corrosion rate ($v_0$ and $v$, g $m^{-2}$ $h^{-1}$) of MS test specimen in $H_2SO_4$ solution without and with various concentrations of GCI-ST were obtained from equation (1), where $m_1$ and $m_2$ are the mass of the specimen before and after corrosion (g), $S$ is the total surface area of the test specimen ($S$=28.0 $cm^2$), $t$ is the immersion time (0-72 h). After $v_0$ and $v$ calculated, the inhibition efficiency ($IE_W$, %)) obtained from this method also can be calculated by equation (2).

$$v = (m_1\text{-}m_2)/St \quad (1)$$

$$IE_W = 100\%\times(v_0\text{-}v)/v_0 \quad (2)$$

*Potentiodynamic polarization measurement:* In this work, the detailed measurement process is described in the literatures [26-27]. Based on this method, the potential sweep rate for Tafel curves was 0.5 mV $s^{-1}$, the inhibition efficiency ($IE_P$, %) can be calculated from equation (3), where $i_{corr}$ and $i_{corr(i)}$ are the corrosion current density (μA $cm^{-2}$) of the MS electrode corrosion in $H_2SO_4$ solution without and with various concentrations of GCI-ST.

$$IE_P = 100\% \times (i_{corr} - i_{corr(i)})/i_{corr} \quad (3)$$

*Microstructure analysis:* Nikon Model Epiphot 200 optical microscope equipped was used to analyze the microstructure of working electrode surface.

## 3. RESULTS AND DISCUSSION

### *3.1 Quantitative analysis of Sinapine thiocyanate*

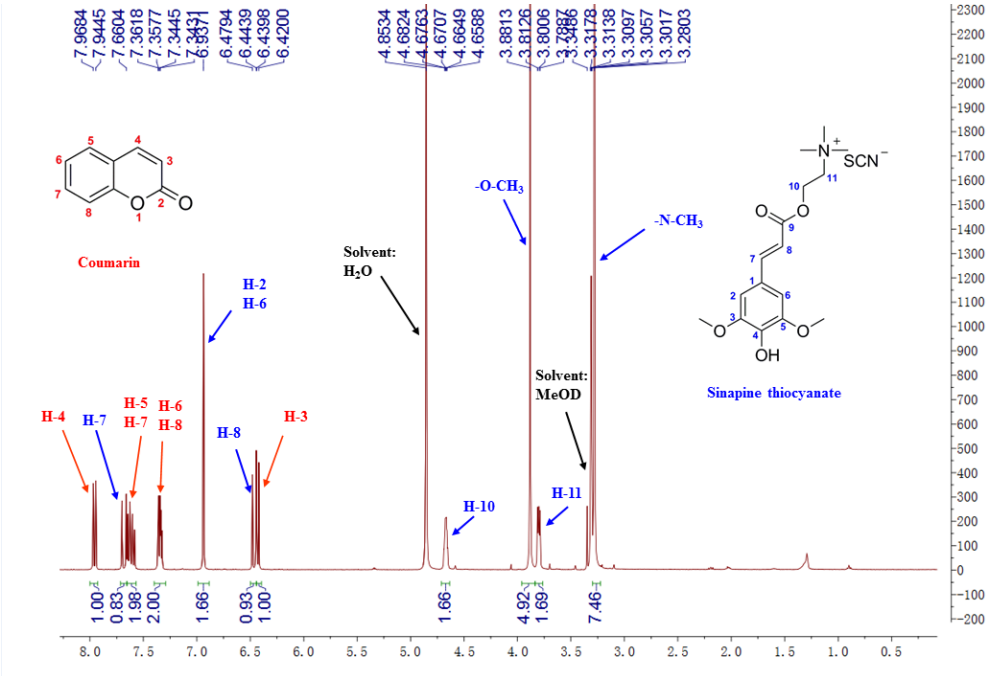


**Figure 2** $^1$H-NMR spectrum of a mixture of *Coumarin* and GCI-ST.

NMR is a well-known analytical method for structure elucidation in academic research. The integral signal intensity in the $^1$H-NMR spectrum is proportional to the number of nuclei and gives information about the quantitative relationship between sample and internal standard substance [28-30]. *Coumarin* was a stable compound and used as an internal reference standard for purity analysis of GCI-ST. *Coumarin* (3.9 mg) and GCI-ST (6.7 mg) were mixed and dissolved in MeOD and recorded with a Bruker Avance-400 spectrometer (400 MHz, Bruker Corporation, Stockholm, Sweden). The $^1$H-NMR spectrum of the mixture of *Coumarin* and GCI-ST is presented in figure 2. Meanwhile, based on this fact of the olefinic proton signals (H-4) of *Coumarin* at 7.95 (1H, d, $J$ = 9.6 Hz) and the aromatic proton signals (H-2, 6) of GCI-ST at 6.94 (1.66H, s) were well separated in the $^1$H-NMR spectrum, the

purity of GCI-ST was calculated by using equation (4). In this equation, $A_s$ is the integral value for GCI-ST, $A_c$ is the integral value for *Coumarin*, $M_s$ is molecular weight of GCI-ST, $M_c$ is the molecular weight of *Coumarin*, $m_s$ is the weight of GCI-ST and $m_c$ is the weight of *Coumarin*. It can be found that the purity of GCI-ST is 96.48%.

$$W_s = (A_s \times M_s \times m_c)/(A_c \times M_c \times m_s) \quad (4)$$

*3.2 Potentiodynamic polarization measurement*

According to potentiodynamic polarization measurement, all the polarization curves (Tafel curves) of MS corrosion in 0.5 M $H_2SO_4$ with various concentrations of GCI-ST at 30°C is presented in figure 3. From this measurement, the inhibition efficiency ($IE_P$, %) and electrochemical parameters including $i_{corr}$ (corrosion current density, $\mu$A cm$^{-2}$), $E_{corr}$ (corrosion potential, mV), $\beta_c$ and $\beta_a$ (cathodic and anodic Tafel slopes, mV dec$^{-1}$) are listed in table 1.

Based on figure 3 and table 1, it can be found that both the anodic and cathodic curves shift to lower current densities after addition of GCI-ST in 0.5 M $H_2SO_4$, which indicates that GCI-ST can reduce the MS anodic dissolution and retard $H^+$ reduction. The results were similar with (2Z,2'Z)-4,4'-((diselanediylbis(4,1-phenylene))bis(azanediyl))bis(4-oxobut-2-enoic acid) and 4,4'-((diselanediylbis(4,1-phenylene))bis(azanediyl))bis(4-oxobutanoic acid) as corrosion inhibitor in acid solution [10]. The inhibition action enhances with the increase of GCI-ST concentration resulting from the adsorption of GCI-ST on MS working electrode surface to form a film, and which can block the MS surface and reduces the corrosive attraction of MS in $H_2SO_4$ solution. Furthermore, according to table 1, it is obvious that $\beta_c$, $\beta_a$, $i_{corr(i)}$ decreases and $IE_P$ increases with GCI-ST concentration increasing. With GCI-ST concentration increase from 20 mg L$^{-1}$ to 600 mg L$^{-1}$, the $IE_P$ also increase from 32.0% to 93.2%, this result reveal that GCI-ST can act as effective corrosion inhibitor for MS in 0.5 M $H_2SO_4$.

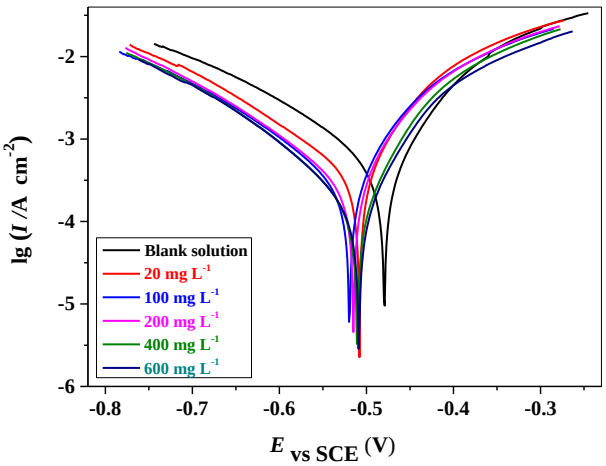


**Figure 3.** Polarization curves of MS in 0.5 M $H_2SO_4$ solution with various concentrations of GCI-ST at 30°C.

In addition, according to the polarization curves showing in figure 3 and the polarization parameters listing in table 1, it can be found that all the $E_{corr}$ of MS corrosion in 0.5 M $H_2SO_4$ with

various concentrations of GCI-ST shift less than 45 mV and slightly in the negative direction. The shift of $E_{corr}$ less than 85 mV indicates that GCI-ST is a mixed-type corrosion inhibitor [31-32].

**Table 1.** Polarization parameters and $IE_P$ of MS in 0.5 M $H_2SO_4$ with various concentrations of GCI-ST at 30°C.

| $c$(mg $L^{-1}$) | $E_{corr}$(mV) | $i_{corr}$ (μA $cm^{-2}$) | $\beta_a$(mV $dec^{-1}$) | $\beta_c$( mV $dec^{-1}$) | $IE_P$(%) |
|---|---|---|---|---|---|
| 0 | 479 | 1075.5 | 101.8 | 145.9 | - |
| 20 | 508 | 731.6 | 111.2 | 141.9 | 32.0 |
| 100 | 515 | 519.6 | 109.0 | 134.1 | 51.7 |
| 200 | 520 | 111.5 | 110.6 | 133.2 | 89.6 |
| 400 | 511 | 89.4 | 94.7 | 119.3 | 91.7 |
| 600 | 507 | 73.1 | 94.3 | 118.4 | 93.2 |

*3.3 Weight loss measurement*

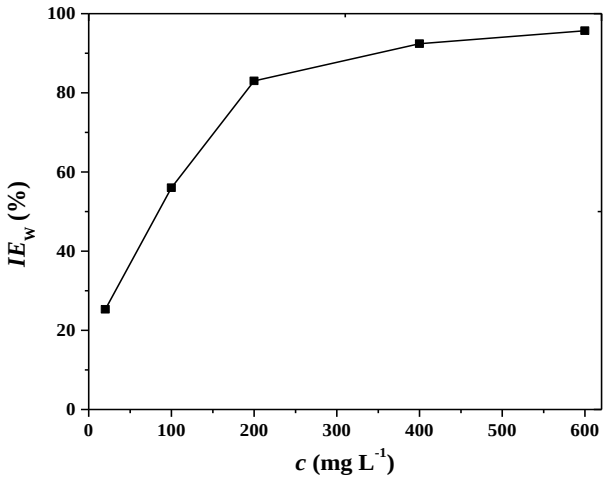


**Figure 4.** The $IE_W$ of MS in 0.5 M $H_2SO_4$ with various concentrations of GCI-ST at 30°C.

The variation of inhibition efficiency ($IE_W$, %) with GCI-ST concentration for MS in 0.5 M $H_2SO_4$ at 30°C is exhibited in figure 4. From this figure, it can be seen clearly that the $IE_W$ remarkable increase with GCI-ST concentration increasing from 20 mg $L^{-1}$ to 400 mg $L^{-1}$, and change slightly with it further increasing. The increase of $IE_W$ is due to more GCI-ST molecules adsorbed on MS surface at the higher concentration, so that the active sites of the MS are protected by GCI-ST molecules. With the concentration of GCI-ST increase to 600 mg $L^{-1}$, the $IE_W$ is 95.7%, this result is in good agreement with the result obtained from potentiodynamic polarization measurement, and further demonstrate that GCI-ST can act as an effective inhibitor for MS in $H_2SO_4$ solution. In addition, compared GCI-ST with other plant extracts including *Date Palm Waste, Sesbania Sesban, Henna, Tobacco Plant, Coriandrum Sativum, Cucumis Sativus, Petroselinum Crispum, Eruca Sativa, Anethum Graveolens*, it can be found that the inhibition efficiency are 84%-89%, 91%, 90.5%, 99%, 85%, 81%, 91%, 93% and 92%, respectively [33]. This compared result also shows that GCI-ST can act as an effective inhibitor.

*3.4 Adsorption isotherm*

From weight loss measurement showing in figure 4, in order to confirm the adsorption isotherm of GCI-ST on MS surface in $H_2SO_4$ solution, different isotherms including Langmuir, Freundlich, Temkin, El-Awady and Flory-Huggins isotherms are employed according to the data of weight loss measurement in this work. The Langmuir adsorption isotherm is presented in equation (5) [8, 26, 34-35]. In this equation, $c$ is the concentration of GCI-ST (20 mg $L^{-1}$ to 600 mg $L^{-1}$). $K$ is the adsorption equilibrium constant. $\theta$ is the surface coverage, which can be obtained by equation (6), where $v_0$ and $v$ obtained by equation (2).

$$c/\theta = 1/K+c \quad (5)$$

$$\theta = (v_0-v)/v_0 \quad (6)$$

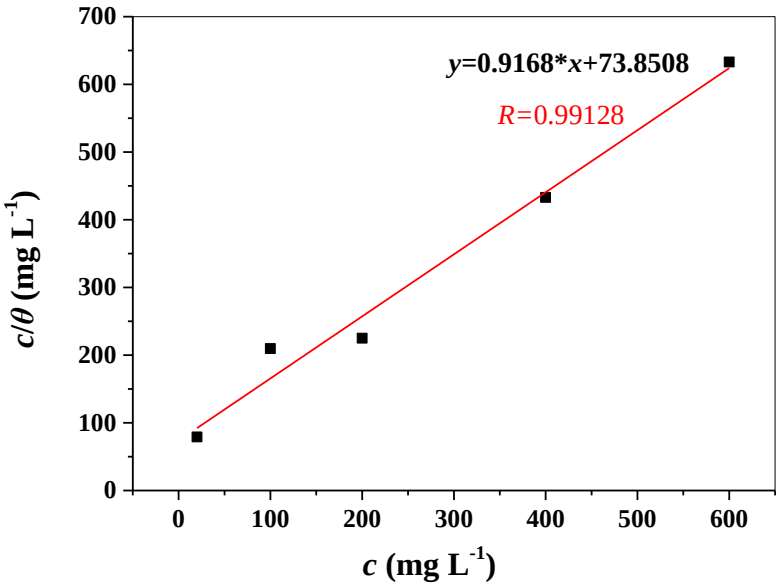


**Figure 5.** Langmuir adsorption isotherm of GCI-ST on MS in 0.5 M $H_2SO_4$.

According to Langmuir adsorption isotherm, the plots of $c/\theta$ versus $c$ yield the straight line shown in figure 5. Based on the fitting result, it can be found that the strong correlation ($R$=0.99128) suggest which the adsorption of GCI-ST on MS surface in 0.5 M $H_2SO_4$ obeys Langmuir adsorption isotherm. And the $\Delta G$ (standard free energy of adsorption) can be determined by equation (7). Where $R$ is the gas constant ($R$=8.314 J $K^{-1}$ $mol^{-1}$), $T$ is absolute temperature (303 K) and 55.5 is the molar concentration of water in the solution expressed in molarity units (mol $L^{-1}$).

$$K = \exp(-\Delta G/RT) \times 1/55.5 \quad (7)$$

Based on equation (7), the calculated values of $\Delta G$ for GCI-ST in 0.5 M $H_2SO_4$ at 30°C is - 31.58 kJ $mol^{-1}$, the value (- 40.00＜ - 31.58 ＜ - 20.00) indicates that the adsorption process of GCI-ST on MS belongs to mixed adsorption involving both physisorption and chemisorption [1, 24, 31].

*3.5 Effect factors*

The effects factors of temperature ($T$, °C), $H_2SO_4$ concentration ($c_{H2SO4}$, M) and storage time ($t$, h) on $IE_W$ obtained from weight loss measurement are presented in figure 6 (a), (b) and (c). From figure 6 (a), as can be seen in 0.5 M $H_2SO_4$ with 600 mg $L^{-1}$ GCI-ST, the $IE_W$ decrease with temperature increasing, with temperature increase from 25°C to 60°C that the $IE_W$ drop from 96.3% to 45.7%. The decrease of $IE_W$ is due to the increase of the temperature might cause desorption of GCI-ST constituents from the surface of MS, and the decrease in the strength of adsorption process at higher temperatures. The similar results were reported by Lai [36] and Gou [37] using S-4-methylbenzyl-O,O'-di(phenyl) dithiophosphate, S-4-methyl benzyl-O,O'-di(4-bromophenyl)dithiophosphate and 5,5,7,12, 12,14-hexamethyl-1,4,8,11-tetraazacyclotetradecane as corrosion in acid solution [36-37].

Meanwhile, figure 6 (b) shows the effect of $c_{H2SO4}$ on $IE_W$ with 600 mg $L^{-1}$ GCI-ST at 30°C. It is obvious that the $IE_W$ decrease with $c_{H2SO4}$ increasing, when the $c_{H2SO4}$ increase from 0.1 M to 4.0 M, the $IE_W$ decrease from 97.1% to 54.9%. The decrease of $IE_W$ is contributed to the higher concentration of $H^+$ resulting from the increase of $H_2SO_4$ concentration. The similar results had been reported by our previous reported [7] using GCI-ST as green corrosion inhibitor for Q235 steel in HCl solution.

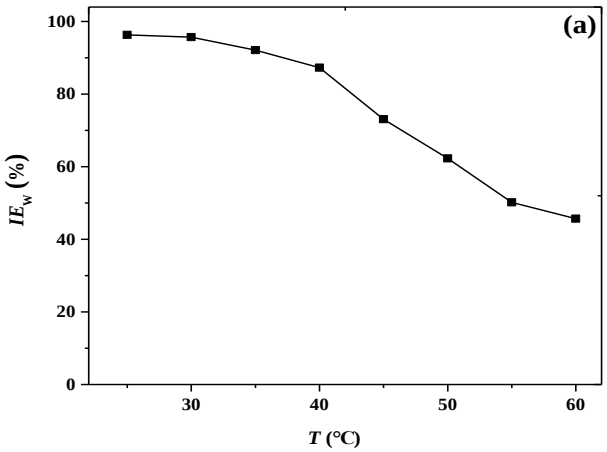


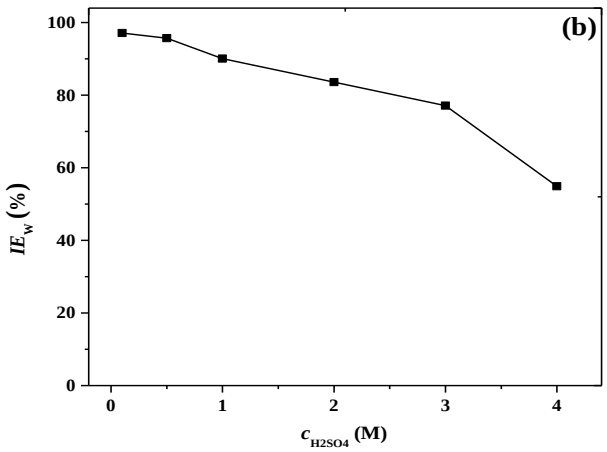

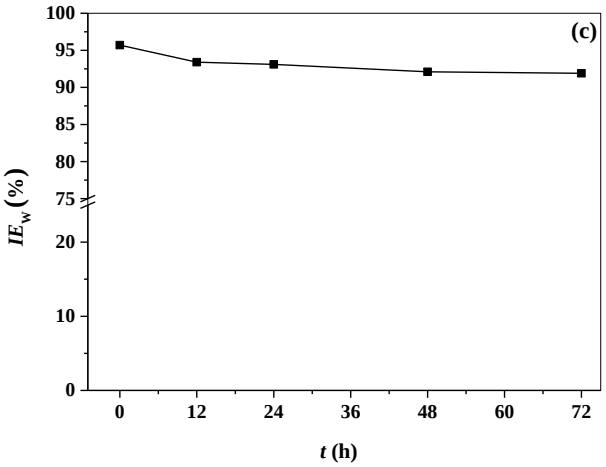


**Figure 6** The effect of temperature (a), $H_2SO_4$ concentration (b) and storage time (c) on $IE_W$ for MS in 0.5 M $H_2SO_4$ with 600 mg $L^{-1}$ GCI-ST.

In addition, based on the effect of storage time on $IE_W$ present in figure 6 (c), it also can be found that $IE_W$ decrease with storage time increasing, which is decreased significantly, especially in 12 hours. After added GCI-ST in 0.5 M $H_2SO_4$ with 600 mg $L^{-1}$ at 12 hours and 72 hours, $IE_W$ decrease from 95.7% to 93.4% and 91.9%, respectively. It concluded that the decrease of $IE_W$ is due to the hydrolysis of the GCI-ST in $H_2SO_4$ solution. Obviously, although GCI-ST was hydrolyzed in 12 hours, the hydrolysis products also exhibited the excellent corrosion inhibition.

*3.6 Microstructure analysis*

For further confirmation of the corrosion inhibition of MS in $H_2SO_4$ solution by GCI-ST, the optical micrographs of MS before and after immersion in 0.5 M $H_2SO_4$ solution without and with 600 mg $L^{-1}$ GCI-ST are presented in figure 7 (a), (b) and (c). From figure 7 (a), it can be seen that the surface morphology of the MS seems smooth with only a few stochastic nicks before immersion in $H_2SO_4$ solution.

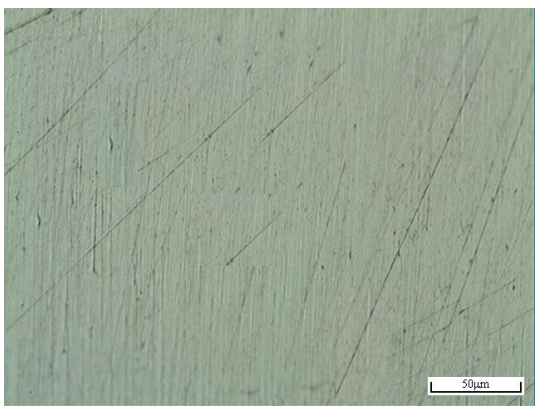


(a)

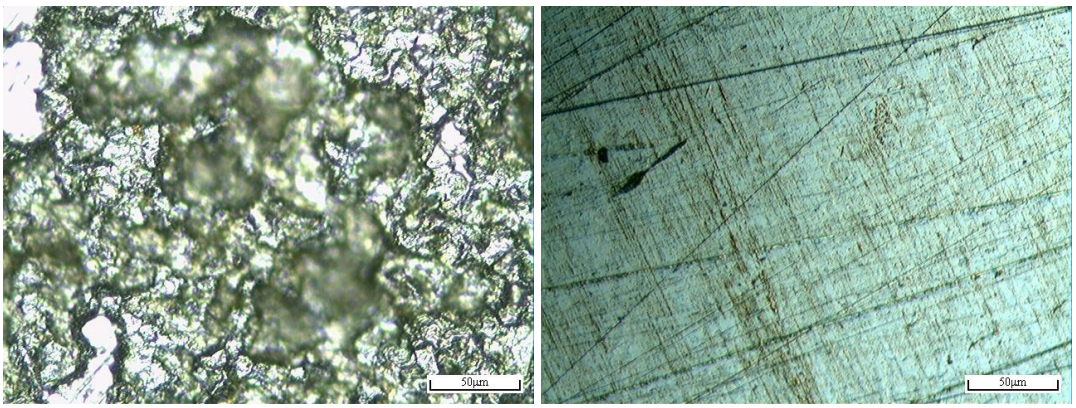


(b) (c)

**Figure 7.** Optical micrographs of MS before and after corrosion in 0.5 $H_2SO_4$: (a) Before corrosion, (b) in 0.5 $H_2SO_4$, (c) in 0.5 $H_2SO_4$ with 600 mg $L^{-1}$ GCI-ST.

However, as can be seen from figure 7 (b), after the MS corrosion 0.5 M $H_2SO_4$ without GCI-ST, which is strongly corroded by $H_2SO_4$ solution. The surface is too bumpy and rough, and there some gullies presented. This result reveals that MS surface is highly corroded by 0.5 M $H_2SO_4$ without GCI-ST. This is in contrast with MS corrosion in 0.5 M $H_2SO_4$ with 600 mg $L^{-1}$ GCI-ST, it also can be found that the MS surface is too smooth and much less damaged (showing in figure 7 (b)), which further confirms the inhibition action and adsorption of GCI-ST on MS surface. Moreover, the microstructure analysis results are in good agreement with the results achieved from the other measurements in this work.

## 4. CONCLUSIONS

(1) The green corrosion inhibitor of GCI-ST was extracted and isolated by *semen raphani* from *Raphanus sativus L.*

(2) GCI-ST can act as an effective corrosion inhibitor for MS in $H_2SO_4$ solution, which is a mixed-type inhibitor.

(3) Inhibition efficiency increase with GCI-ST concentration increasing, decrease with temperature, $H_2SO_4$ concentration and storage time increasing.

(4) The adsorption of GCI-ST on MS surface obeys Langmuir isotherm, which belongs to the mixed adsorption involving both chemisorption and physisorption.

ACKNOWLEDGEMENTS
This project is supported financially by the program of Education Department of Sichuan Province (No. 18ZB0514) and the Projects of Key Laboratories of Fine Chemicals and Surfactants in Sichuan Provincial Universities (No. 2016JXZ03).

## References

1. R.H. Albrakaty, N.A. Wazzan and I.B. Obot, *Int. J. Electrochem. Sci.*, 13 (2018) 3535.
2. J. Bhawsar, P. Jain, M.G. Valladares-Cisneros, C. Cuevas-Arteaga and M.R. Bhawsar, *Int. J. Electrochem. Sci.*, 13 (2018) 3200.

3. C. Kamal and M.G. Sethuraman, *Ind. Eng. Chem. Res.*, 51 (2012) 10399.
4. K.H. Hassan, A.A. Khadom, and N.H. Kurshed, *S. Afr. J. Chem. Eng.*, 22 (2016) 1.
5. I.H. Ali and M.H.A. Suleiman, *Int. J. Electrochem. Sci.*, 13 (2018) 3910.
6. J. Bhawsar, P.K. Jain and P. Jain, *Alex. Eng. J.*, 54 (2015) 769.
7. X.L. Jiang, C. Lai, Z. Xiang, Y.F. Yang, B.L. Tan, Z.Q. Long, L.P. Liu, Y.T. Gu, W.J. Yang and X. Chen, *Int. J. Electrochem. Sci.*, 13 (2017) 3234.
8. U.M. Eduok, S.A. Umoren and A.P. Udoh, *Arab. J. Chem.*, 5 (2012) 325.
9. N.O. Obi-Egbedi, I.B. Obot and S.A. Umoren, *Arab. J. Chem.*, 5 (2012) 361.
10. R. Vera, F. Figueredo, A. Díaz-Gómez and A. Molinari, *Int. J. Electrochem. Sci.*, 13 (2018) 4139.
11. National Pharmacopoeia Committee. Pharmacopoeia of the People's Republic of China. Beijing: *China Medical Science press*.1 (2015) 272.
12. Y.B. Li and S. Jing, *Inf. Tradit. Chin. Med.*, 27 (2010) 8.
13. P.Q. Kuang, D. Song, Q.P. Yu, R. Yi, X.H. Lv and H. Liang, *Food. Chem.*, 136 (2013) 342.
14. Y. Hu, H. Liang, Q.P. Yuan and Y.C. Hong, *Nat. Prod. Res.*, 24 (2010) 1195.
15. H. Liang, Q.P. Yuan, H.R. Dong, Z.M. Qian and Y.M. Liu, *Chin. Pharmacol. J.*, 39 (2004) 898.
16. J. Schmidt, T. Yokota, G. Adam and N. Takahashi, *Phytochemistry*, 30 (1991) 364.
17. J. Schmidt, T. Yokota, B. Spengler and G. Adam, *Phytochemistry*, 34 (1993) 391.
18. M.F. Zhang and Y.Q. Shen, *Pharmacol. Clin. Chin. Mater. Med.*, 1 (1996) 29.
19. B. Matthäus, *Food. Chem.*, 50 (2002) 3444.
20. F.Q. Guo, Q. Li and R.Q. Gu, *J. Rad. Res. Rad. Pro.*, 13 (1995) 177.
21. W. Y. Li, Q. Li, F. Q. Guo and R. Q. Gu, *Acta. Phytophy. Sin.*, 23 (1997) 319.
22. Q. Li and R.Q. Gu, *Chin. J. Appl. Environ. Biol.*, 5 (1999) 32.
23. Q. Li and R.Q. Gu, *Am. J. Plant Sci.*, 1 (2010) 113.
24. L. Boucherit, T. Douadi, N. Chafai, M. Al-Noaimi and S. Chafaa, *Int. J. Electrochem. Sci.*, 13 (2018) 3997.
25. A.S. Fouda, S.H. Etaiw and M. Salah, *Int. J. Electrochem. Sci.*, 13 (2018) 4670.
26. L. Saqalli, M. Galai, N. Gharda, M. Sahrane, R.Ghailane, M.E. Touhami, Y. Peres-lucchese, A. Souizi and N. Habbadi, *Int. J. Electrochem. Sci.*, 13 (2018) 5096.
27. E.E. El-Katori and Y.M.A. Angari, *Int. J. Electrochem. Sci.*, 13 (2018) 4319.
28. S.K. Bharti and R. Roy, *Trac-trend. Anal. Chem.*, 35 (2012) 5.
29. F. Malz and H. Jancke, *J. Pharmaceut. Biomed.*, 38 (2005) 813.
30. S.K. Chauthe, R.J. Sharma, F. Aqil, R.C. Guptab and I.P. Singh, *Phytochem. Analysis*, 15 (2012) 689.
31. Y. Qiang, S. Zhang, S. Yan, X. Zou and S. Chen, *Corros. Sci.*, 127 (2017) 295.
32. M.P. Casaletto, V. Figà, A. Privitera, M. Bruno, A. Napolitano and S. Piacente, *Corro. Sci.*, 136 (2018) 91.
33. G. M. Al-Senani and M. Alshabanat, *Int. J. Electrochem. Sci.*, 13 (2018) 3777.
34. M.H.O. Ahmed, A.A. Al-Amiery, Y.K. Al-Majedy, A.A.H. Kadhum, A.B. Mohamad and T.S. Gaaz, *Res. Phys.*, 8 (2018) 728.
35. K.F. Khaled and S.S. Abdel-Rehim, *Arab. J. Chem.*, 4 (2011) 397.
36. C. Lai, X. Guo, J. Wei, B. Xie, L. Zou, X. Li, Z. Chen andC. Wang, *Open Chem.*, 15 (2017) 163.
37. W. Gou, C. Lai, Z. Xiang, L. Yang, P. Zhang, W. Xie, L. Chen, G. Luo, X. Li, Z. Chen, *Int. J. Electrochem. Sci.*, 12 (2017) 11742.